Available online at www.sciencedirect.com

SciVerse ScienceDirect

Applied Mathematical modelling (2015)

APPLIED MATHEMATICAL MODELLING

www.elsevier.com/locate/apm

A 8-Neighbour Model Lattice Boltzmann Method Applied to Mathematical-Physical Equations

Bo AN[a], J.M. Bergadà[b]

[a]Univeridad politécnica de Madrid, Escuela Técnica Superior de Ingenieros Aeronáuticos.Madrid,20852, Spain
[b]Univeritat Politècnica de Catalunya, BarcelonaTech, ESEIAAT-UPC Colom, 11 08222 Terrassa, Spain

Abstract

A lattice Boltzmann method (LBM) 8-neighbour model (9-bit model) is presented to solve mathematical-physical equations, such as, Laplace equation, Poisson equation, Wave equation and Burgers equation. The 9-bit model has been verified by several test cases. Numerical simulations, including 1D and 2D cases, of each problem are shown respectively. Comparisons are made between numerical predictions and analytic solutions or available numerical results from previous researchers. It turned out that the 9-bit model is computationally effective and accurate for all different mathematical-physical equations studied. The main benefits of the new model proposed is that it is faster than the previous existing models and has a better accuracy.

Keywords: 8-neighbour model, (9-bit model), lattice Boltzmann method, Mathematical-physical equations

1. Introduction

Lattice Boltzmann method (LBM) is a relatively new alternative of computational fluid mechanics. It was generated and developed from lattice gas automata (LGA) [1]-[3] and the kinetic theory of Boltzmann equation [4]-[5]. This method has been studied and researched for over 30 years since it was born, and it gradually became a hot topic worldwide. LBM is based on the mechanism of gas molecules. But, it is different from the traditional numerical methods. Besides, it is a discrete method in macroscopic scale, while, a continuous method in microscopic scale [6]. It is known that LBM can be employed in many research fields, such as microscopic flow [7], crystal growth [8], magnetic fluid [9]-[10], biological fluid [11]-[12], porous media flows [13]-[15], turbulence [16]-[17], burning chambers [18], multiphase flows [19]-[20], micro-nanoscopic and non-equilibrium flows[21]-[22], non-Newtonian and transcritical flows [23]-[24] etc., where the traditional numerical methods are very difficult to be applied. Many scholars have made great contributions in simulating mathematical-physical equations, such as, Laplace equation, Poisson equation, wave equation, Burgers equation, KdV equation, Schrödinger equation, Euler equation and N-S equation. The aim of this paper is to construct a series of 9-bit models as an inheritance and improvement of those predecessors' work [25]-[32]. Zhang et al, presented a 5-bit model in their work [28], this model works well in dealing with the Laplace equation. Chai and Shi presented a lattice Boltzmann model to solve the 2D and 3D

Corresponding author. Tel.: +34 691173315; fax: +34 937398101.
E-mail address: bo_alan_an@163.com (BO AN)

Poisson equations [25], in the model they presented there was a genuine solver to the Poisson equation, the transient term was eliminated. For 2D Poisson equation, they developed a 5-bit model, which was tested by numerical cases. In 2000, Yan [27] developed a lattice Boltzmann model for 1D and 2D wave equations with truncation error of order two. In his paper, the author presented a 5-bit model and a 9-bit model with tested numerical cases. In his model, it is not necessary to have an ensemble average to get the macroscopic quantity, so the statistical errors disappear. Duan and Liu [26] developed a special lattice Boltzmann model to simulate 2D unsteady Burgers equation. The maximum principle and the stability were proved in their work. Their study indicates that lattice Boltzmann model is highly stable and efficient even for the problems with severe gradient. This model is a 4-bit model without the stationary state in discrete velocities. They developed another lattice Boltzmann model to solve the modified Burgers equation in 2008 [30]. In this new paper, they presented a 2-bit model without stationary state in discrete velocities for 1D modified Burgers equation. Zhang and Yan [32] proposed a higher-order moment lattice Boltzmann method for 1D and 2D Burgers equation. In order to achieve higher order accuracy, they used seven and four moments of the equilibrium distribution functions in 1D and 2D models respectively. In their paper, they presented a 5-bit model with verified numerical cases.

Nomenclature

c	The lattice sound speed
$C0_\alpha$	Coefficients to be determined
$C1_\alpha$	Coefficients to be determined
$C2_\alpha$	Coefficients to be determined
$\vec{e}_\alpha$	Unit velocities vector along discrete directions
$f(u)$	Source term in mathematical-physical equations
F_α	Out-force term of lattice Boltzmann equation
$F_\alpha^{(2)}$	Multiple scale expansion term of out-force term of lattice Boltzmann equation
$f(\vec{r},t)$	Distribution functions
f_α	Discrete distribution functions
$f_\alpha^{(1)}$	Multiple scale expansion term of discrete distribution functions around f_α^{eq}
$f_\alpha^{(2)}$	Multiple scale expansion term of discrete distribution functions around f_α^{eq}
f_α^{eq}	The equilibrium state of discrete distribution functions
f_α^{neq}	The non-equilibrium state of discrete distribution functions
$\vec{r}$	Space position vector
$\vec{r}_b$	Space position vector of point $\boldsymbol{b}$
$\vec{r}_f$	Space position vector of point $\boldsymbol{f}$

$\vec{r}_{ff}$	Space position vector of point ***ff***
$\vec{r}_{w}$	Space position vector of point ***w***
Re	Reynolds number
t	Time
t_1	Expansion term of time scale
t_2	Expansion term of time scale
t_0	Present time step used in fourth order Runge-Kutta scheme
u	Macroscopic quantities in mathematical-physical equations
u^{t_0}	u of present time step
$u^{t_0+\Delta t}$	u of next time step
$k_{1,2,3,4}$	Parameters of fourth order Runge-Kutta scheme
α	Discrete directions
β	A parameter of wave equation to be determined
Δ_e	Embed depth
Δt	Time step
Δx	Grid spacing
ε	Small Knudsen number
λ	A parameter to be determined
ν	Kinematic viscosity coefficient
σ_{ij}	Kronecker symbol
τ	Single relaxation time
ω_α	Weight coefficient
$\bar{\omega}_\alpha$	Weight coefficient in Chai's model
∇^2	Laplace operator
∇u	Gradient of macroscopic quantity u
∇	Partial differential operator
∇_1	Space expansion term of partial differential operator

Superindices

αi	α represents discrete directions and $i=1,2$ represents the coordinates in x and y directions
αj	α represents discrete directions and $j=1,2$ represents the coordinates in x and y directions
eq	Represents equilibrium
neq	Represents no-equilibrium

2. Lattice Boltzmann Method

In 1988, Mcnamara and Zanetti presented the earliest lattice Boltzmann model [2]. In their model, the evolution equation of lattice gas automata was replaced by Boltzmann equation. Since then (1988), many efforts have been done to improve and develop the lattice Boltzmann method in order to increase its numerical stability, accuracy, applicability and other numerical properties. In 1989, Higuera and Jimenez proposed a simplified model [33] via introducing the equilibrium distribution function, which linearize the collision operator. In the same year, Higuera et al. proposed an improved model [34] with the enhanced collision operator to improve the numerical stability of the model itself. These two models above eliminated the statistical noise of the lattice gas automata and overcame the complexity of collision operator.

In 1991, Chen et al. advanced a single-relaxation-time model [9], simplifying the collision operator even further. In 1992, Qian et al. presented a similar method called LBGK model [35], the model in their work was based on the collision theory [36] presented by Bhatnagar, Gross and Krook, which is aiming to simplify the complex collision term in the Boltzmann equation. Besides, many researchers have developed new models like multiple-relaxation-time LB model and regularized LB model. In 2001, d'Humières developed the multiple-relaxation-time LB model, in his work [37], he demonstrated the superior numerical stability of the multiple-relaxation-time lattice Boltzmann equation over the popular lattice BGK equation. Recently, Li et al. [38] used a double MRT model to simulate 3D fluid with heat transfer, it turned out this double MRT model had a good performance in 3D natural convection numerical simulations. Latt et al. [39], presented the regularized LB model, where they proved that the new scheme was both more accurate and stable in the hydrodynamic regime. Montessori et al. [40], investigated the accuracy and performance of the regularized version of the single-relaxation-time lattice Boltzmann equation. As a numerical methodology, LBM has been well developed in many aspects, nowadays, thanks to researchers' contributions, LBM can be successfully applied to many research fields. Regarding future LBM perspectives, Succi [41] predicted some possibilities for the next 25 years.

In the present approach, the variables $f(\vec{r},t)$ are defined as the particles distribution function. The lattice Boltzmann BGK equation is defined as

$$f_\alpha(\vec{r}+\vec{e}_\alpha\Delta t, t+\Delta t)-f_\alpha(\vec{r},t)=\frac{1}{\tau}[f_\alpha(\vec{r},t)-f_\alpha(\vec{r},t)] \tag{1}$$

This equation is the same as the one previously used by other researchers in order to solve Navier-Stokes equations [35]. Regarding the definition of macroscopic quantities used in the present paper, equation 2(a) is given to define u in Laplace-Poisson and Burgers equations, equation 2(b) defines the term $\frac{\partial u}{\partial t}$ in wave equation.

The macroscopic quantities u and $\frac{\partial u}{\partial t}$ are defined as

$$\begin{cases} u = \sum_{\alpha} f_{\alpha} & (a) \\ \dfrac{\partial u}{\partial t} = \sum_{\alpha} f_{\alpha} & (b) \end{cases} \tag{2}$$

To satisfy the conservation condition, it is assumed

$$u = \sum_{\alpha} f_{\alpha} = \sum_{\alpha} f_{\alpha}^{eq} \tag{3}$$

For simplicity, the macroscopic quantity u is defined in a general way in all target equations. However, this variable u characterizes a different physical meaning in each equation. Notice that all equations and variables presented in the present paper are non-dimensional. These three equations above, which were also used by other researchers [25]-[32], are the keystone equations in solving mathematical-physical equations with LBM.

Being a numerical methodology, like other kinds of traditional computational methods, lattice Boltzmann method also needs research of stability analysis. In 1996, J.D. Sterling et al. [42] presented an analysis of the stability of lattice Boltzmann models with a 7-velocity hexagonal lattice, a 9-velocity square lattice, and a 15-velocity cubic lattice. In their work [42], they proved that, for lattice BGK model, the single relaxation term τ must be greater than 0.5. In 2006, M.K. Banda et al. [43] introduced a stability analysis requirement for the lattice Boltzmann method and derived some relations of parameters for several lattice Boltzmann models. The present 9-bit model introduced in this paper, can be characterized by the same stability analysis of the lattice Boltzmann method [42, 43] introduced above. Since the discrete velocities lattice employed in the present paper is the same as the one used in [42, 43].

3. Recovering The Target Equations From LBE

In this section, the target equations are recovered from the lattice Boltzmann equation, and the equilibrium distribution functions are constructed for each mathematical-physical equation studied in this paper.

Figure 1 presents the two dimensional 9-bit model where the discrete velocities $\vec{e}_{\alpha}$ are introduced, the term ω_{α}, called the weight coefficients applied in the 9-bit model, is also presented.

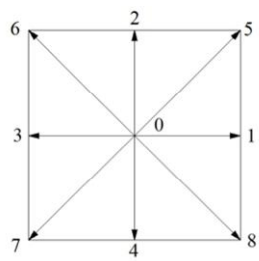

$$\begin{cases} \vec{e}_{\alpha} = (0,0), \alpha = 0 \\ \vec{e}_{\alpha} = c(\cos[(\alpha-1)\frac{\pi}{2}], \sin[(\alpha-1)\frac{\pi}{2}]), \alpha = 1,2,3,4 \\ \vec{e}_{\alpha} = c(\cos[(2\alpha-1)\frac{\pi}{4}], \sin[(2\alpha-1)\frac{\pi}{4}]), \alpha = 5,6,7,8 \end{cases}$$

$$\omega_{\alpha} = [\frac{4}{9}, \frac{1}{9}, \frac{1}{9}, \frac{1}{9}, \frac{1}{9}, \frac{1}{36}, \frac{1}{36}, \frac{1}{36}, \frac{1}{36}] \ (\alpha = 0,\ldots,8)$$

Fig. 1. Introduces the two dimensional 9-bit model, which describes the discrete velocities, where ω_α are the weight coefficients applied in the 9-bit model.

3.1. Laplace-Poisson Equations

The target equation is written as

$$\nabla^2 u = f(u) \tag{4}$$

where $f(u)$ is the source term that is zero for the Laplace equation. If it is not zero, the equation becomes the Poisson equation. In order to recover the target equation from the LBE the following assumptions were considered

$$\begin{cases} \sum_\alpha f_\alpha^{eq} = u \\ \sum_\alpha f_\alpha^{eq} \vec{e}_\alpha = 0 \\ \sum_\alpha f_\alpha^{eq} \vec{e}_{\alpha i} \vec{e}_{\alpha j} = \lambda u \sigma_{ij} \end{cases} \tag{5}$$

where $\vec{e}_{\alpha i}(i=1,2)$ represent the unit velocities vector along discrete directions and $i=1,2$ denotes x or y directions in 2-dimensional Cartesian coordinates.

The lattice Boltzmann equation (LBE), with out-force term, is given by

$$f_\alpha(\vec{r}+\vec{e}_\alpha \Delta t, t+\Delta t) - f_\alpha(\vec{r},t) = -\frac{1}{\tau}[f_\alpha(\vec{r},t) - f_\alpha^{eq}(\vec{r},t)] + \Delta t F_\alpha \tag{6}$$

F_α is the out-force term of lattice Boltzmann equation. Via implementing the out-force term, the relation between this term and the source term of equation (4) can be obtained. This relation will allow to recover the Laplace-Poisson equation from lattice Boltzmann equation, allowing as well to solve both equations via using the present 9-bit model.

With the use of second-order Taylor expansion to the equation above, it is obtained

$$\Delta t(\frac{\partial}{\partial t} + \vec{e}_\alpha \cdot \nabla) f_\alpha + \frac{\Delta t^2}{2}(\frac{\partial}{\partial t} + \vec{e}_\alpha \cdot \nabla)^2 f_\alpha = -\frac{1}{\tau}(f_\alpha - f_\alpha^{eq}) + \Delta t F_\alpha \tag{7}$$

Via using the multi-scale expansion given in [36, 44], the following equations can be derived.

$$\begin{cases} f_\alpha = f_\alpha^{eq} + \varepsilon f_\alpha^{(1)} + \varepsilon^2 f_\alpha^{(2)} \\ F_\alpha = \varepsilon F_\alpha^{(2)} \\ \nabla = \varepsilon \nabla_1 \\ \frac{\partial}{\partial t} = \varepsilon^2 \frac{\partial}{\partial t_2} \end{cases} \tag{8}$$

where ε is a small Knudsen number and $\nabla = \frac{\partial}{\partial x_i}$ is the partial differential operator, where $x_i (i = 1,2)$ denote x or y directions in 2-dimensional Cartesian coordinates.

Introducing equations (8) into equation (7). The equation to the first order of ε is presented as:

$$\varepsilon^1 : \Delta t \vec{e}_\alpha \cdot \nabla_1 f_\alpha^{eq} = -\frac{1}{\tau} f_\alpha^{(1)} \tag{9}$$

The equation to the second order of ε is called ε^2 and takes the form:

$$\varepsilon^2 : \frac{\partial}{\partial t_2} f_\alpha^{eq} + \vec{e}_\alpha \cdot \nabla_1 f_\alpha^{(1)} + \frac{\Delta t}{2} (\vec{e}_\alpha \cdot \nabla_1)^2 f_\alpha^{eq} = -\frac{1}{\tau \Delta t} f_\alpha^{(2)} + F_\alpha^{(2)} \tag{10}$$

Performing the operation $\varepsilon \times$ equation (9) $+ \varepsilon^2 \times$ equation (10), the following equation is obtained

$$\frac{\partial}{\partial t} f_\alpha^{eq} + \Delta t \vec{e}_\alpha \cdot \nabla f_\alpha^{eq} + (0.5 - \tau) \Delta t (\vec{e}_\alpha \cdot \nabla)^2 f_\alpha^{eq} = -\varepsilon \frac{1}{\tau} f_\alpha^{(1)} + F_\alpha \tag{11}$$

It must be noticed that in equation (11), u is time independent. Summarizing equation (11), it is obtained

$$\Delta t (0.5 - \tau) \lambda \nabla^2 u = \sum_\alpha F_\alpha \tag{12}$$

where λ is a parameter to be determined.

Then the Laplace-Poisson equation has been recovered as

$$\nabla^2 u = f(u) \tag{13}$$

Hence, it is obtained that $F_\alpha = \omega_\alpha f(u)(0.5 - \tau) \Delta t \lambda$.

At this point it is assumed that the equilibrium distribution function has the following form

$$f_\alpha^{eq} = C0_\alpha u + C1_\alpha u^2 + C2_\alpha u^3 \tag{14}$$

$C0_\alpha$, $C1_\alpha$ and $C2_\alpha$ are coefficients to be determined.

Empirically, in order to close the system, it is necessary to introduce some artificial complementary conditions which are given by

$$\begin{cases} C0_1 = C0_2 = C0_3 = C0_4 \\ C0_5 = C0_6 = C0_7 = C0_8 \\ C0_1 = 4C0_5 \end{cases} \tag{15}$$

Introducing equation (5) and equation (15) into equation (14), the equilibrium distribution function is obtained.

$$\begin{cases} f_0^{eq} = (1-\dfrac{5}{3c^2})\lambda u \\ f_{1,2,3,4}^{eq} = \dfrac{u}{3c^2}\lambda \\ f_{5,6,7,8}^{eq} = \dfrac{u}{12c^2}\lambda \end{cases} \tag{16}$$

Where $c = \Delta x/\Delta t$. Notice that the present 9-bit model is capable of solving the Laplace and Poisson equation in a general way, which is different from the 5-bit model presented in Zhang's et al work [28], where the equilibrium distribution function was given by the following equation

$$\begin{cases} f_{1,2,3,4}^{eq} = \dfrac{1}{2}\lambda u \\ f_0^{eq} = (1-2\lambda)u \end{cases} \tag{17}$$

It is also different from the model presented in Chai's work [25], where the equilibrium distribution function was given by the following equation

$$\begin{cases} f_\alpha^{eq} = (\bar{\omega}_\alpha - 1)u, \quad \alpha = 0 \\ f_\alpha^{eq} = \bar{\omega}_\alpha u, \quad \alpha = 1,2,3,4 \end{cases} \tag{18}$$

3.2. Burgers Equations

The Burgers equation is a fundamental partial differential equation in fluid mechanics. It is written as

$$\frac{\partial u}{\partial t} + u\nabla u + \nu\nabla^2 u = 0 \tag{19}$$

where $\nu = 1/Re$.

Following the process described in the previous section, it is defined f_α as the particle distribution function with discrete directions denoted by α. In order to recover the Burgers equation from the LBE, the following assumptions are considered

$$\begin{cases} \sum_\alpha f_\alpha^{eq} = u \\ \sum_\alpha f_\alpha^{eq} \vec{e}_\alpha = \dfrac{u^2}{2} \\ \sum_\alpha f_\alpha^{eq} \vec{e}_{\alpha i} \vec{e}_{\alpha j} = \lambda u \sigma_{ij} \end{cases} \tag{20}$$

The macroscopic quantity u and conservative condition are defined in the same way as presented in the former section. The LBE without the out-force term is the one to be used in the present case, which is equation (6) without the out-force term, the last term.

By using second order Taylor expansion and multiple expansion technology, it is obtained

$$\begin{cases} f_\alpha = f_\alpha^{eq} + \varepsilon f_\alpha^{(1)} + \varepsilon^2 f_\alpha^{(2)} \\ \dfrac{\partial}{\partial t} = \varepsilon^2 \dfrac{\partial}{\partial t_2} \\ \nabla = \varepsilon \nabla_1 \end{cases} \tag{21}$$

The equation to the first order of ε is given as:

$$\varepsilon^1 : \vec{e}_\alpha \cdot \nabla_1 f_\alpha^{eq} + \frac{1}{\tau \Delta t} f_\alpha^{(1)} = 0 \tag{22}$$

The equation to the second order of ε, ε^2 takes the form:

$$\varepsilon^2 : \frac{\partial}{\partial t_2} f_\alpha^{eq} + \vec{e}_\alpha \cdot \nabla_1 f_\alpha^{(1)} + \frac{\Delta t}{2} (\vec{e}_\alpha \cdot \nabla_1)^2 f_\alpha^{eq} + \frac{1}{\tau \Delta t} f_\alpha^{(2)} = 0 \tag{23}$$

When introducing equation (22) into equation (23), the following equation is obtained

$$\frac{\partial}{\partial t_2} f_\alpha^{eq} + \Delta t (0.5 - \tau)(\vec{e}_\alpha \cdot \nabla_1)^2 f_\alpha^{eq} + \frac{1}{\tau \Delta t} f_\alpha^{(2)} = 0 \tag{24}$$

Performing the following operation $\varepsilon \times$ equation (22) + $\varepsilon^2 \times$ equation (24), the next equation is reached

$$\frac{\partial}{\partial t} f_\alpha^{eq} + \vec{e}_\alpha \cdot \nabla f_\alpha^{eq} + \frac{\varepsilon}{\tau \Delta t} f_\alpha^{(1)} + \varepsilon^2 \Delta t (0.5 - \tau)(\vec{e}_\alpha \cdot \nabla_1)^2 f_\alpha^{eq} = 0 \tag{25}$$

Summarizing equation (25), it is obtained the following equation given by

$$\frac{\partial u}{\partial t} + \nabla \frac{u^2}{2} + \lambda (0.5 - \tau) \Delta t \nabla^2 u = 0 \tag{26}$$

Then, the Burgers equation has been recovered and given by

$$\frac{\partial u}{\partial t} + u \nabla u + \nu \nabla^2 u = 0 \tag{27}$$

where $\nu = \lambda (0.5 - \tau) \Delta t$ and τ is the single relaxation time.

In the same way, it is assumed that the equilibrium distribution function has the form given by equation (14). Again, the following two equations are some empirical manmade conditions required to close the system of equations.

$$\begin{cases} C0_1 = C0_2 = C0_3 = C0_4 \\ C0_5 = C0_6 = C0_7 = C0_8 \\ C0_1 = 4C0_5 \end{cases} \tag{28}$$

$$\begin{cases} C1_1 = C1_2 = -C1_3 = -C1_4 \\ C1_5 = C1_6 = -C1_7 = -C1_8 \\ C1_1 = 4C1_5 \end{cases} \tag{29}$$

Introducing equation (20), (28) and (29) into equation (14), the equilibrium distribution function is addressed as follows

$$\begin{cases} f_0^{eq} = (1-\dfrac{5\lambda}{6c^2})u \\ f_{1,2}^{eq} = \dfrac{\lambda}{6c^2}u + \dfrac{u^2}{10c} \\ f_{3,4}^{eq} = \dfrac{\lambda}{6c^2}u - \dfrac{u^2}{10c} \\ f_{5,6}^{eq} = \dfrac{\lambda}{24c^2}u + \dfrac{u^2}{40c} \\ f_{7,8}^{eq} = \dfrac{\lambda}{24c^2}u - \dfrac{u^2}{40c} \end{cases} \tag{30}$$

It is to be highlighted that equation (30) is different from the equilibrium distribution function presented in reference [32], where the equilibrium distribution function was written in the following form.

$$\begin{cases} f_0^{eq} = (1-\dfrac{2\lambda}{c^2})u - \dfrac{2u^3}{3c^2} \\ f_{1,2}^{eq} = \dfrac{\lambda u}{2c^2} + \dfrac{u^2}{4c} + \dfrac{u^3}{6c^2} \\ f_{3,4}^{eq} = \dfrac{\lambda u}{2c^2} - \dfrac{u^2}{4c} + \dfrac{u^3}{6c^2} \end{cases} \tag{31}$$

For 1D case, the model presented in [30] was addressed as:

$$\begin{cases} f_1^{eq} = \dfrac{u}{2c^2} + \dfrac{u^2}{4c} \\ f_2^{eq} = \dfrac{u}{2c^2} - \dfrac{u^2}{4c} \end{cases} \tag{32}$$

3.3. Wave Equations

Here is the last application presented in this paper. The target equation is written as

$$\frac{\partial^2 u}{\partial t^2} = \beta \nabla^2 u + f(u) \tag{33}$$

where $f(u)$ is called the source function because in practice it describes the effects of the sources of waves on the medium carrying them and β is a parameter of wave equation to be determined. When $f(u)$ equals zero, the target equation becomes the wave equation we are familiar with. Otherwise, this equation is called inhomogeneous wave equation. Following the same procedure previously described, it is defined the macroscopic quantity $\frac{\partial u}{\partial t}$ as [27]

$$\frac{\partial u}{\partial t} = \sum_{\alpha} f_{\alpha} \tag{34}$$

The conservative condition is the same as that of equation (3). In order to recover the wave equation from LBE, the same assumptions as the ones described by equation (5) were used. Introducing the LBE with out-force term and using the second order Taylor expansion and multiple scale expansion, it is reached

$$\begin{cases} f_{\alpha} = f_{\alpha}^{eq} + \varepsilon f_{\alpha}^{(1)} + \varepsilon^2 f_{\alpha}^{(2)} \\ F_{\alpha} = \varepsilon F_{\alpha}^{(2)} \\ \nabla = \varepsilon \nabla_1 \\ \frac{\partial}{\partial t} = \varepsilon \frac{\partial}{\partial t_1} + \varepsilon^2 \frac{\partial}{\partial t_2} \end{cases} \tag{35}$$

The first order equation of ε takes the form:

$$\varepsilon^1 : (\frac{\partial}{\partial t_1} + \vec{e}_{\alpha} \cdot \nabla_1) f_{\alpha}^{eq} + \frac{1}{\tau \Delta t} f_{\alpha}^{(1)} = 0 \tag{36}$$

The second order equation of ε, named ε^2 is given as:

$$\varepsilon^2 : \frac{\partial}{\partial t_2} f_{\alpha}^{eq} + (\frac{\partial}{\partial t_1} + \vec{e}_{\alpha} \cdot \nabla_1) f_{\alpha}^{(1)} + \frac{\Delta t}{2} (\frac{\partial}{\partial t_1} + \vec{e}_{\alpha} \cdot \nabla_1)^2 f_{\alpha}^{eq} + \frac{1}{\tau \Delta t} f_{\alpha}^{(2)} = F_{\alpha}^{(2)} \tag{37}$$

Introducing equation (36) into equation (37), the following equation is obtained.

$$\frac{\partial}{\partial t_2} f_{\alpha}^{eq} + \Delta t (0.5 - \tau) (\frac{\partial}{\partial t_1} + \vec{e}_{\alpha} \cdot \nabla_1)^2 f_{\alpha}^{eq} + \frac{1}{\tau \Delta t} f_{\alpha}^{(2)} = F_{\alpha}^{(2)} \tag{38}$$

Building the following operation $\varepsilon \times$ equation (36) + $\varepsilon^2 \times$ equation (38), it is reached.

$$\frac{\partial}{\partial t} (\frac{\partial u}{\partial t}) + (0.5 - \tau) \Delta t \nabla^2 f_{\alpha}^{eq} e_{\alpha} e_{\alpha} = \sum_{\alpha} F_{\alpha} \tag{39}$$

Hence, the wave equation has been recovered as

$$\frac{\partial^2 u}{\partial t^2} - \beta \nabla^2 u = f(u) \tag{40}$$

where $\beta = \lambda(\tau - 0.5)\Delta t$ and $F_\alpha = \omega_\alpha f(u)$.

As already done in the two previous target equations, it is assumed that the equilibrium distribution function has the form given by equation (14). In order to close the system, some artificial conditions are introduced and written as equation (15). For Wave equations, the assumption defined in equation (5) is now modified as the following equation.

$$\begin{cases} \sum_\alpha f_\alpha^{eq} = \dfrac{\partial u}{\partial t} \\ \sum_\alpha f_\alpha^{eq} \vec{e}_\alpha = 0 \\ \sum_\alpha f_\alpha^{eq} \vec{e}_{\alpha i} \vec{e}_{\alpha j} = \lambda u \sigma_{ij} \end{cases} \tag{41}$$

Introducing equation (41) and equation (15) into equation (14), it is obtained:

$$\begin{cases} f_0^{eq} = \dfrac{\partial u}{\partial t} - \dfrac{5}{3c^2}\lambda u \\ f_{1,2,3,4}^{eq} = \dfrac{u}{3c^2}\lambda \\ f_{5,6,7,8}^{eq} = \dfrac{u}{12c^2}\lambda \end{cases} \tag{42}$$

Comparing the present case with the model presented in Yan's work [27], where the equilibrium distribution function was addressed as equation (43), it can clearly be seen that the distribution functions are different from the previous ones presented in this paper.

$$\begin{cases} f_0^{eq} = \dfrac{\partial u}{\partial t} - \dfrac{2}{c^2}\lambda u, \quad \alpha=0 \\ f_\alpha^{eq} = \dfrac{u}{4c^2}\lambda, \quad \alpha=1,2,3,4,5,6,7,8 \end{cases} \tag{43}$$

For the wave equations, the conservative condition is given as:

$$\frac{\partial u}{\partial t} = \sum_\alpha f_\alpha = \sum_\alpha f_\alpha^{eq} \tag{44}$$

After each evolution of lattice Boltzmann equation, the new value of $\frac{\partial u}{\partial t}$ is obtained. In order to solve u for next time step, the fourth order Runge-Kutta scheme was used. The scheme is written as:

$$\begin{cases} u^{t_0+\Delta t} = u^{t_0} + \dfrac{1}{6}(k_1 + k_2 + k_3 + k_4) \\ k_1 = \Delta t \dfrac{\partial u}{\partial t}(t_0, u^{t_0}) \\ k_2 = \Delta t \dfrac{\partial u}{\partial t}(t_0 + 0.5\Delta t, u^{t_0} + 0.5k_1) \\ k_3 = \Delta t \dfrac{\partial u}{\partial t}(t_0 + 0.5\Delta t, u^{t_0} + 0.5k_2) \\ k_4 = \Delta t \dfrac{\partial u}{\partial t}(t_0 + \Delta t, u^{t_0} + k_3) \end{cases} \quad (45)$$

where t_0 is the initial time, u^{t_0} is u for the present time step, $u^{t_0+\Delta t}$ is u for the next time step and $k_{1,2,3,4}$ are parameters in fourth order Runge-Kutta scheme.

4. Boundary Conditions

The treatment of boundary conditions is very important to numerical simulations of computational fluid mechanics, and it has a big influence on computational results. In this section, the treatment of boundary conditions involved in this paper is presented.

4.1. Straight Wall Boundary Condition

The non-equilibrium extrapolation scheme presented in [45] is employed to treat the straight wall boundary condition in the current numerical simulations. The general idea of this scheme is that the distribution function of each direction can be classified into two parts, known as the non-equilibrium part and the equilibrium part.

Figure 2 is presenting the boundary condition for straight boundaries involved in the present numerical cases, it has to be noticed that points ***A***, ***B***, ***C*** characterize the flow points, while points ***D***, ***E***, ***F***, define the wall boundaries.

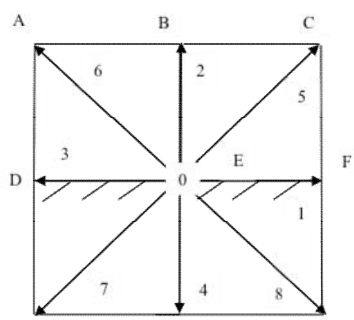

Fig. 2 introduces the straight wall boundary condition, where points ***A***, ***B*** and ***C*** are flow points, while points ***D***, ***E*** and ***F*** are wall boundary points.

Taking the point ***E*** for example, the distribution functions of each direction are written as

$$f_\alpha(E,t) = f_\alpha^{eq}(E,t) + f_\alpha^{neq}(E,t) \tag{46}$$

With the non-equilibrium extrapolation scheme, Eq. (46) becomes

$$f_\alpha(E,t) = f_\alpha^{eq}(E,t) + (1-\frac{1}{\tau})[f_\alpha(B,t) - f_\alpha^{eq}(B,t)] \tag{47}$$

4.2. Curved Wall Boundary Condition

For curved wall boundaries, figure 3, the unknown parts of distribution functions can be determined through a special linear interpolation.

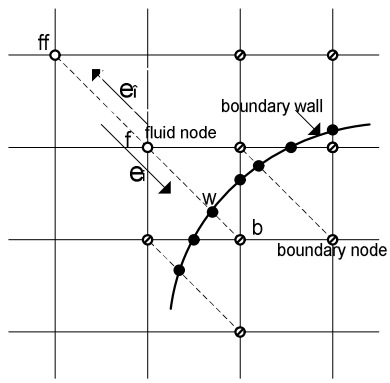

Fig. 3 presents the straight wall boundary condition, point ***ff*** and point ***f*** belong to flow points, while point ***w*** is a wall boundary point and point ***b*** is an internal wall point (virtual point).

Taking the point ***f*** for example, only the distribution function of direction 6 (shown in Fig.1), addressed as f_6, is unknown after the first evolution process. In Chen et al paper [46], they presented an accurate curved boundary treatment, which is also used in the present paper. Taking the point ***b*** for example, after each evolution, the equilibrium distribution function of point ***f*** along direction 6 is unknown and constructed as

$$f_6(\vec{r}_f, t+\Delta t) = f_6(\vec{r}_w, t+\Delta t) + \frac{\Delta_e}{1+\Delta_e}[f_6(\vec{r}_{ff}, t+\Delta t) - f_6(\vec{r}_w, t+\Delta t)] \tag{48}$$

where: $\Delta_e = \dfrac{\left|\vec{r}_f - \vec{r}_w\right|}{\left|\vec{r}_f - \vec{r}_b\right|}$.

However, the distribution function of point ***w*** along direction 6 is also unknown. According to the non-slip condition, it is obtained the following form to address the distribution function of point ***w*** along direction 6.

$$f_6(\vec{r}_w, t+\Delta t) = f_8(\vec{r}_w, t+\Delta t) \tag{49}$$

The distribution function of point ***w*** along direction 8 (shown in Fig.1) is obtained through a linear interpolation and written as the following form

$$f_8(\vec{r}_w, t+\Delta t) = f_8(\vec{r}_f, t+\Delta t) + \Delta_e[f_8(\vec{r}_b, t+\Delta t) - f_8(\vec{r}_f, t+\Delta t)] \tag{50}$$

Introducing equations (49) and (50) into (48), the distribution functions of the point ***b*** along direction 6 is obtained. As a result of this development, the streaming operation, from the point ***b*** to the point ***f***, can be smoothly finished. In the present research, Mei et al scheme [47] and Guo et al scheme [48] were also evaluated, it turned out they all work well with the curved wall boundaries.

5. Test Cases

In this section different numerical cases will be evaluated, the 9-bit model proposed in this paper will be tested and compared with the previous models or with the analytical solutions. The benefits of the present model will be highlighted, indicating why this model should be seen as an advanced one for the cases studied.

Case 1.

In this case the 2D Laplace equation is simulated in a square zone, the test equation is written as

$$\begin{cases} \nabla^2 u = 0 \ (0 \le x \le 1, \ 0 \le y \le 1) \\ u(x,0) = 0, \ u(x,1) = \sin(\pi x) \\ u(0,y) = u(1,y) = 0 \end{cases} \tag{51}$$

The exact solution presented in Zhang's work [28], is $u(x,y) = \dfrac{\sin(\pi x)\sinh(\pi y)}{\sinh(\pi)}$, where they also presented a 5-bit model for 2D Laplace equation.

Figure 4 introduces the comparison between the 9-bit model presented in this paper and the exact solution already presented in Zhang's work. The figure on the left, represents the variable u obtained via numerical prediction of the present 9-bit model by using a 100×100 mesh size, with constants designed as c=1.0, τ=1.5, and λ=0.5. Notice that the agreement is good.

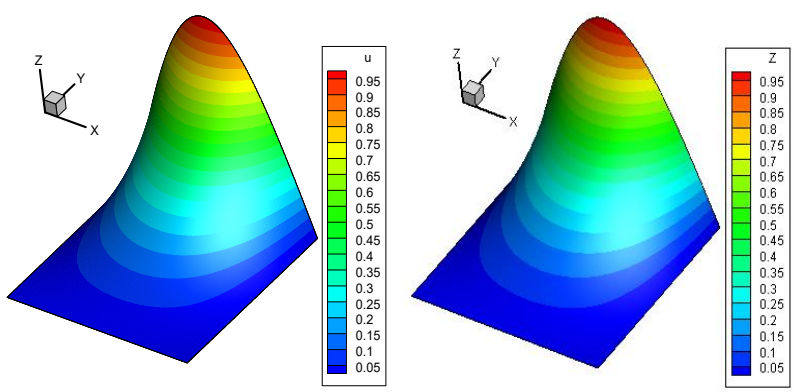

Fig. 4. Compares 3D view of the numerical prediction of the present 9-bit model, left hand side, with the exact solution of 2D Laplace equation, right hand side. Mesh size was 100×100, c=1.0, τ=1.5, λ=0.5 and contour number is 15.

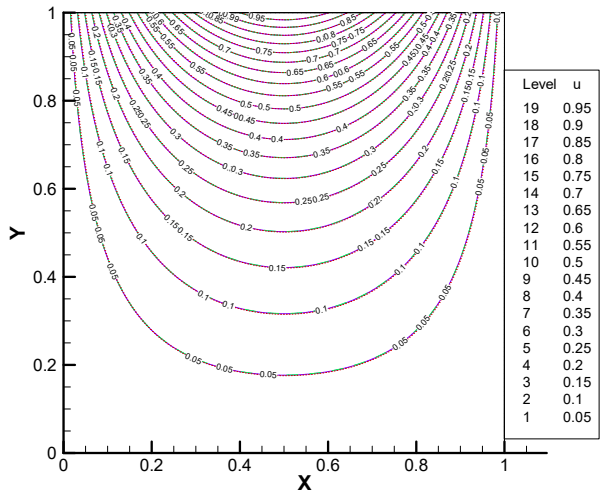

Fig. 5. Comparison between the prediction of this paper, numerical result of Zhang et al [28] model and exact solution. Mesh size was 100×100, c =1.0, τ =1.5, λ =0.5 and contour number is 15.

Since figure 4 is just giving an overall view of the comparison, to further evaluate the model performance, it is required a 2D projected view between the analytical results, Zhang's et al ones [28] and the 9-bit model introduced in the present paper, such view is presented in figure 5. The solid purple line represents the analytic solution, the dashed green line is the result of Zhang's et al model [28] and the dotted red line is the prediction of the present research. Notice that the three results are almost identical, the small maximum differences are presented in table 2.

In the present case, three different mesh sizes were evaluated, 50×50, 100×100 and 200×200, for the three cases, the parameters c =1.0, τ =1.5, λ =0.5 and contour number = 15, were kept constant.

Table 1 presents the comparison between the computational time required for the present model and Zhang et al model. Comparison is being made for three different grid sizes. Notice that independently of the grid size used, the 9-bit model introduced in this paper, is converging faster. The ratio (t1/t2) is the computational time between reference [28] model and the present 9-bit model. Table 2 introduces the maximum error obtained when comparing the exact solution with the one obtained by Zhang's et al model and the present 9-bit model, regardless of the grid size used, the actual model is producing a smaller error than the Zhang's et al one. At this point, it is important to clarify that to obtain all tables presented in all different cases evaluated, except table 7, the models developed by previous researchers as well as the 9-bit model introduced in this paper, were programmed and computed on the same computer, being the boundary conditions identical, therefore the results obtained are fully comparable and just depend on the model itself. The results presented in table 7, were taken directly from the data given by previous researchers.

Table 1. t1 is the time that consumed by 5-bit model [28], t2 is the counterpart that of 9-bit model presented in this paper.

Mesh size	Data source	Convergence condition	Ratio (t1/t2)
(50,50)	Present paper	10(-6)	2.174
	Ref.28(5-bit)	10(-6)	
(100,100)	Present paper	10(-6)	2.115
	Ref.28(5-bit)	10(-6)	
(200,200)	Present paper	10(-6)	2.019
	Ref.28(5-bit)	10(-6)	

Table 2. The comparison of maximum value of error with different resolutions between 9-bit model and Zhang et al model [28].

Mesh size	Data source	Maximum error	Convergence condition
(50,50)	Ref.28(5-bit)	0.00037896	10(-6)
	Present paper	0.0002135	10(-6)
(100,100)	Ref.28(5-bit)	0.000247	10(-6)
	Present paper	0.000136	10(-6)
(200,200)	Ref.28(5-bit)	0.001035	10(-6)
	Present paper	0.0010153	10(-6)

As a conclusion from tables 1 and 2, it can be said that the 9-bit model is computationally efficient and accurate.

Case 2.

In this case the 2D Laplace equation is simulated in a curved zone, the aim of this case is to prove that the 9-bit model presented in this paper is capable of solving the 2D Laplace equation with curved boundaries, the test equation is written as

$$\begin{cases} \nabla^2 u = 0 \\ u(x,y) = \sin(\pi y)\cos(\pi x) \\ (x,y) \in x^2 + y^2 = 1 \end{cases} \tag{52}$$

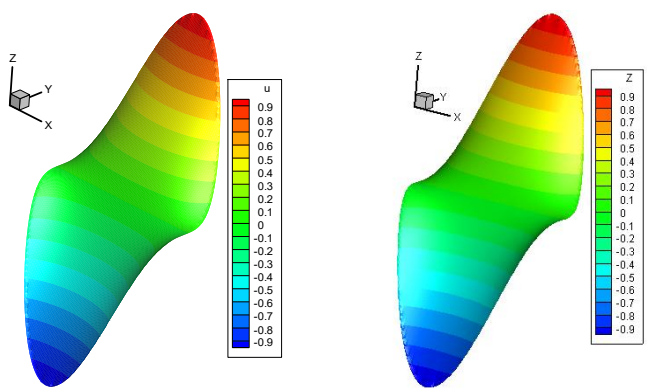

Fig. 6. 3D view of 2D Laplace equation in case 2. The variable u at the left side is calculated by using 9-bit model presented in this paper. The variable Z at the right side is numerical solution calculated by finite-difference methods (FDM).

Considering the target equation (52), it is difficult to get the analytic solution. Hence, the numerical solution, calculated by finite-difference method, with convergence condition 10(-10) is introduced to substitute the analytic solution. For simplicity, the numerical solution calculated by FDM will be addressed as analytic solution in this case. Figure 6 presents the 3D view of 2D Laplace equation obtained using the actual 9-bit model, left hand side, the comparison with numerical solution calculated by finite-difference method, is presented on the right hand side. Both figures show exactly the same results. Figure 7 introduces the 2D plain view plot of figure 6. The solid green line represents the analytic solution and the dotted red line is the prediction of this paper. As can be seen from figure 7, the numerical result shows a very good agreement with the analytic solution.

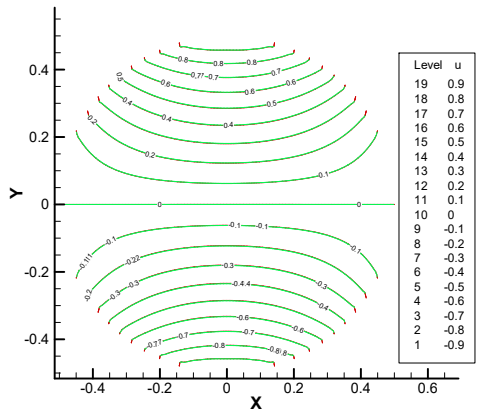

Fig. 7. Comparison between the prediction of this paper and exact solution.

The mesh used was a non-uniform Cartesian grid, having 8649 cells. The parameters were c=1.0, τ =1.2, λ=1/2 and the contour number was 15. The disk diameter employed was 1.

Table 3 introduces the comparison between the computational time obtained by Zhang et al [28] model and the present model, it also presents the maximum error generated by these two models when compared with the exact solution. Results show that the present 9-bit model is computationally efficient and accurate when solving 2D Laplace equation with curved boundary.

Table 3. The comparison between 9-bit model and Zhang's 5-bit model. t1 is the time that consumed by 5-bit model [28], t2 is the counterpart that of 9-bit model presented in this paper.

Model	Mesh size	Maximum error	Convergence condition	t1/t2
5-bit Zhang [28]	8649	0.003977	10(-6)	1.58
9-bit	8649	0.001408	10(-6)	

Case 3.

In this case the 2D Poisson equation is simulated in a square zone, the test equation is written as

$$\begin{cases} \nabla^2 u = -2\pi^2 \cos(\pi x)\sin(\pi y) \\ 0 \le x \le 1, 0 \le y \le 1 \\ u(x,0) = u(x,1) = 0 \\ u(0,y) = \sin(\pi y),\ u(1,y) = -\sin(\pi y) \end{cases} \tag{53}$$

The analytic solution is $u(x,y) = \cos(\pi x)\sin(\pi y)$.

Figure 8, left hand side, presents the 3D view of 2D Poisson equation obtained using the present 9-bit model, for comparison, the analytic solution is to be found on the right hand side. The figure shows that the numerical prediction and the analytical solution are almost identical. Nevertheless, in order to closely compare these results, figure 9 is presented.

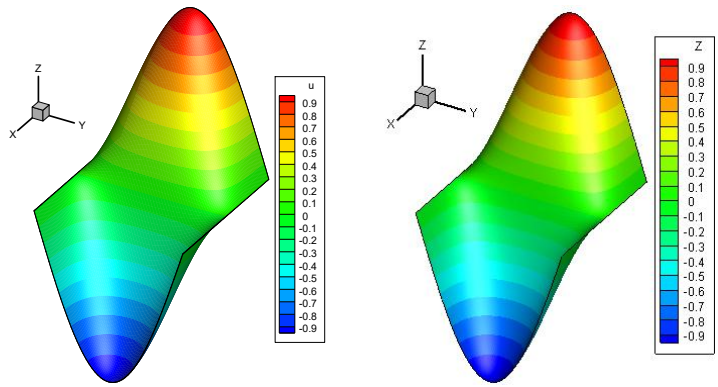

Fig. 8. 3D view of 2D Poisson equation in case 3. The variable u at the left side is calculated by using 9-bit model presented in this paper. The variable Z at the right side is the exact solution. Mesh size was 100×100, c =1.0, τ =1.1, λ =0.5 and contour number is 15.

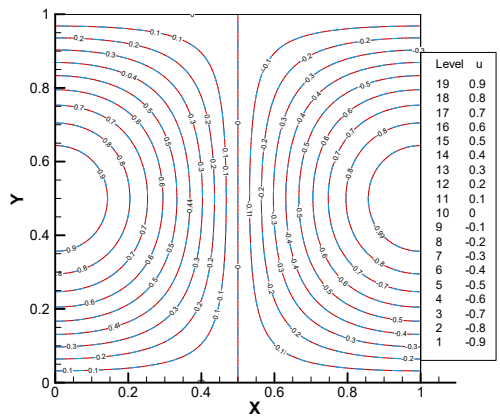

Fig. 9. Comparison between the prediction of this paper and exact solution. Mesh size was 100×100, c =1.0, τ =1.1, λ =0.5 and contour number is 15.

Figure 9 introduces the 2D plain view plot of figure 8. The solid red line represents the analytic solution and the dotted blue line is the prediction from this paper. In order to show the advantage of the actual 9-bit model, the Zhang's et al 5-bit model was further developed in this paper to deal with Poisson equation, because the original one could only be applied to solve the Laplace equation. Table 4 presents the comparison between the computational time obtained by the 5-bit modified model from Zhang's et al. and the current model. Table 5 presents the maximum error generated by the current model and the 5-bit modified Zhang's et al. model, when compared with the exact solution. In both tables, the comparisons were done for three different mesh sizes.

Table 4. t1 is the time that consumed by 5-bit model, t2 is the counterpart that of 9-bit model presented in this paper.

Mesh size	Data source	Convergence condition	Ratio (t1/t2)
(50,50)	9-bit	10(-6)	1.413
	5-bit	10(-6)	
(100,100)	9-bit	10(-6)	1.399
	5-bit	10(-6)	

(200,200)	9-bit	10(-6)	1.380
	5-bit	10(-6)	

Table 5. The comparison of maximum value of error with different resolutions between 9-bit model and 5-bit model

Mesh size	Data source	Maximum error
(50,50)	Modified Zhang's 5-bit	0.000315
	Present 9-bit	0.000337
(100,100)	Modified Zhang's 5-bit	0.000255
	Present 9-bit	0.000128
(200,200)	Modified Zhang's 5-bit	0.000755
	Present 9-bit	0.000534

From tables 4 and 5, it can be seen that the 9-bit model is computationally efficient and accurate when solving the 2D Poisson equation, yet, a small particularity was found when evaluating the (50, 50) resolution. For this particular case, the modified Zhang's 5-bit model, presented a slightly smaller error than the 9-bit model one. The authors believe that the reason behind this mismatch, could be connected with the fact that a 9-bit model is a very accurate one, and the (50, 50) resolution grid is too coarse to show any advantage of the present model over a lower level model.

Case 4.

In this case, the 2D wave equation will be simulated, the test equation is written as

$$\begin{cases} \dfrac{\partial^2 u}{\partial t^2} = \beta\ \nabla^2 u + f(x,y,t) \\ (x,y) \in (0,1)\times(0,1),\ t \geq 0 \end{cases} \tag{54}$$

where $\beta = 1$. The boundary and initial conditions are

$$\begin{cases} u(0,y,t) = u(1,y,t) = 0 \\ u(x,0,t) = u(x,1,t) = 0 \\ u(x,y,0) = x(1-x)y(1-y) \\ \dfrac{\partial u}{\partial t}(x,y,0) = 0 \end{cases} \tag{55}$$

and the source term is given as the following equation

$$f(x,y,t) = (2x - 2x^2 + 2y - xy + x^2 y - 2y^2 + xy^2 - x^2 y^2)\cos(t) \tag{56}$$

For this case, the analytical solution is taking the following form:

$$u(x,y,t) = x(1-x)y(1-y)\cos(t) \tag{57}$$

Figure 10, on the left hand side, presents the 3D view of the solution of equation (54) at time equals 0.2, calculated by the current 9-bit model, the right hand side shows the analytical solution for the same time. Figure 11 is the projected view of figure 10, the solid red line represents the analytical solution and the dotted black line represents the prediction of this paper, it shows that the prediction presented in this paper has a

good agreement with the exact solution, indicating that the 9-bit model proposed in this paper is able to accurately solve the 2D Wave equation.

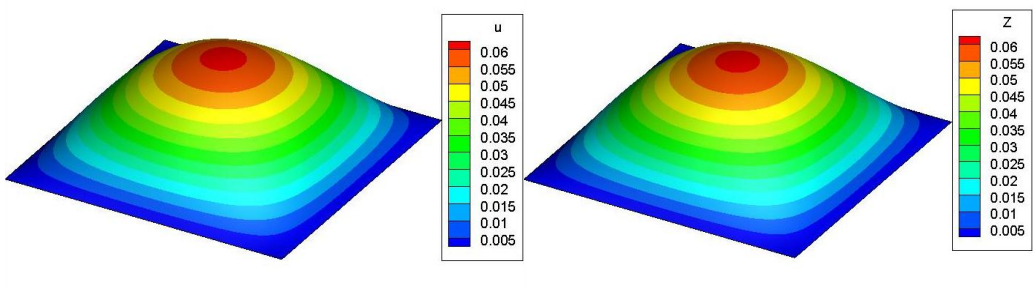

Fig. 10. Calculated u in 3D view at time $t=0.2$. Mesh size was 100×100, $c=5.0$, $\tau=1.2$, $\beta=1.0$ and contour number is 15. Actual 9-bit model, left hand side, and analytical solution, right hand side.

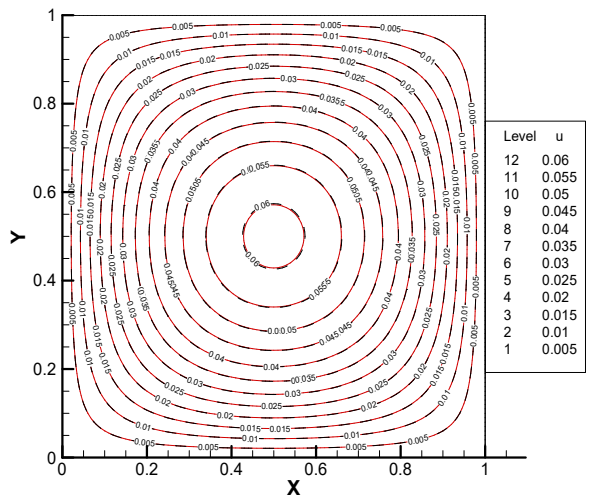

Fig. 11. Comparison between the prediction of this paper and exact solution at time $t=0.2$. Mesh size was 100×100, $c=5.0$, $\tau=1.2$, $\beta=1.0$ and contour number is 15.

In order to further compare the accuracy of the present model, Yan's models [27], were programmed to solve this particular case. Table 6 introduces the maximum error generated by the current model and Yan's [27] 5-bit and 9-bit models when compared with the exact solution. It is noticed from table 6 that the 9-bit model presented in this paper produces smaller errors than these two models.

Table 6. The comparison of maximum value of error with different resolutions between present 9-bit model and Yan's 5-bit and 9-bit model [27].

Mesh size	Data source	Maximum error	Convergence condition
(100,100)	Present 9-bit model	0.000086	10(-6)
	Yan's 9-bit model	0.007712	10(-6)
	Yan's 5-bit model	0.000090	10(-6)

Case 5.

For the present case, the 1D Burgers equation is to be evaluated, case 5 is designed to compare the lattice Boltzmann model presented in this paper with other traditional (CFD) methods [49] and [50]. The 1D Burgers equation was chosen due to its simplicity to implement it computationally.

The test equation is written as

$$\frac{\partial u}{\partial t}+u\frac{\partial u}{\partial x}=\nu\frac{\partial^2 u}{\partial x^2} \tag{58}$$

According to [49, 50], $\nu=0.01/\pi$ and the boundary and initial conditions are

$$\begin{cases} u(x,0)=-\sin(\pi x) \\ -1\le x\le 1 \\ u(-1,t)=u(1,t)=0 \end{cases} \tag{59}$$

Figure 12 presents the solution of equation (58) for different time, as expected, the slope of the curve increases as time increases. The left side of figure 12 introduces the results calculated based on the model presented in this paper, and the right side presents the numerical results obtained in Vassilis's work [49]. From figure 12, it can be seen that the two results are almost the same, especially when considering the tendency of the slope with time increase. In order to compare the present results with the ones obtained by [49] and [50], it is typically used the curve slope at time equals 0.5. From Vassilis [49] and Macaraeg and Streett work [50], the values of the slope at time $t=0.5$ were respectively 152.0052 and 152.0049. In the present work and for the same time, it is found that the value of the slope is 152.0067. As a conclusion it can be stated that the present lattice Boltzmann model is able to solve 1D Burgers equation.

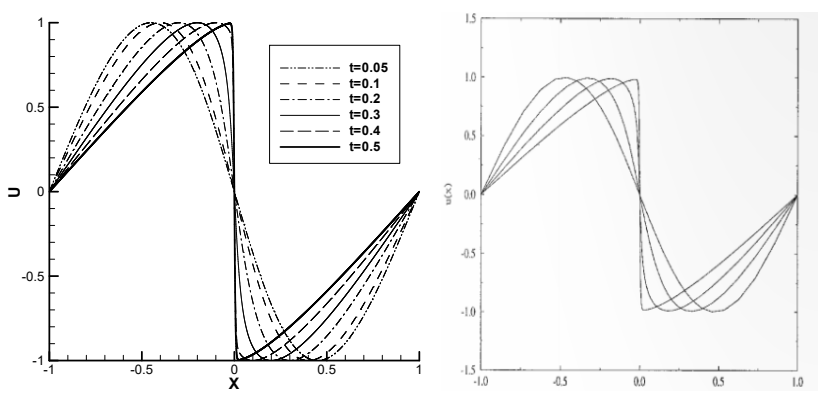

Fig. 12. The lines represent the numerical prediction at different time. The mesh size is 100, c =5.0, τ =1.5.

Case 6.

For the present case, the 1D modified Burgers equation is to be evaluated, the test equation is written as

$$\frac{\partial u}{\partial t}+u^2\frac{\partial u}{\partial x}=\nu\frac{\partial^2 u}{\partial x^2} \tag{60}$$

According to [30], $\nu = 0.01$ and the boundary and initial conditions are

$$\begin{cases} u(x,0) = -\sin(\pi x) \\ 0 \le x \le 1 \\ u(0,t) = u(1,t) = 0 \end{cases} \tag{61}$$

Figure 13 introduces the solution of equation (60) when using the present model for different non-dimensional times, ranging from 0.5 to 2.5. The left hand side of figure 13 presents the numerical prediction of this paper and the right hand side of figure 13 introduces the results computed in reference [30]. It can be seen from figure 13 that the two results are nearly the same.

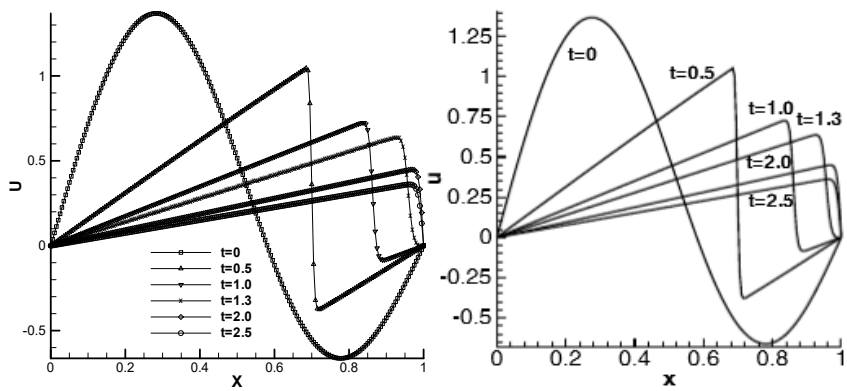

Fig. 13. Shows the value of *u* calculated in this paper at different time.

Table 7. Comparison of the value of *u* at different position along coordinate *x* at *t*=2.0.

Coordinate x	Present paper	Ref.20	Ref.35
0.10	0.11179	0.11194772	0.11013979
0.20	0.20683	0.20710153	0.20614825
0.30	0.28477	0.28512152	0.28477813
0.40	0.34997	0.35038171	0.35045112
0.50	0.40619	0.40665374	0.40700602
0.60	0.45598	0.45649486	0.45704614
0.70	0.50092	0.50155303	0.50224419
0.80	0.54138	0.54199420	0.54265295
0.90	0.534529	0.53547356	0.53225529

In order to further validate the results obtained from the previous simulations, table 7 was created. It can be seen that the comparison has been made between the results calculated by present model, the results proposed in reference [30] and the results presented in reference [51], where the collocation method with quantic splines was applied. It is found that the present model is capable of solving the 1D modified Burgers equation and the numerical results are acceptable when compared with the two other computed results.

6. Conclusions

In this paper, a lattice Boltzmann method 9-bit model is presented, and applied to a series of 1D and 2D

mathematical-physical equations. Several test cases are presented to compare the 9-bit model and numerical predictions generated in this paper, with the work undertaken by previous researchers or with analytic solutions. In all cases studied, the 9-bit model performed well. Some main conclusions are summarized below.

- New equilibrium distribution functions were derived for the present 9-bit model to solve each target equation, see equations, 16, 30 and 42.
- To match with the discrete velocities lattice, the artificial constrains were chosen, they were the same for all cases evaluated and different from previous researchers work.
- It turns out that the present 9-bit model is numerically more effective and accurate in solving the studied target equations than the previous models evaluated.
- Numerical results show that the 9-bit model is capable of solving 2D problems with both straight and curved geometries. It also solves 1D problems.
- This 9-bit model can solve the Laplace-Poisson and wave equation, which are recovered from LBE, in a general way, by introducing the out-force term. The relation between the out-force term and the source term is to be seen as different versus the previous existing ones.

Acknowledgements

The first author of this paper wishes to express his gratitude to Professor SANG Weimin. Thanks to his generous assistance, the present paper could be accomplished.

References

[1] U. Frisch, B. Hasslacher, and Y. Pomeau, “Lattice-gas automata for the Navier-Stokes equation,” Phys. Rev. Lett. 56, 1505-1508 (1986).
[2] G.R. McNamara, “Use of the Boltzmann to simulate lattice automata,” Phys. Rev. Lett. 61, 2322-2335 (1988).
[3] Dieter A. Wolf-Gladrow, “Lattice-Gas Cellular Automata and Lattice Boltzmann Models,” Lecture Notes in Mathematics. 1725 (2000).
[4] X.Y. He, S.Y. Chen, and G.D. Doolen, “A novel thermal model for the lattice Boltzmann method in incompressible limit,” Journal of Computational Physics. 146, 1, 283-300 (1998).
[5] S. Succi, “Lattice Boltzmann equation for fluid dynamics and beyond,” Oxford: Clarendon Press (2001).
[6] H. Yaling, W. Yong, and L. Qing, “Lattice Boltzmann method: Theory and applications,” Science Press (2008).
[7] D. Raabe, “Overview of the lattice Boltzmann method for nano- and microscale fluid dynamics in materials science and engineering,” Modelling and Simulation in Materials Science and Engineering. 12, 13-46 (2004).
[8] W. Miller, and S. Succi, “A Lattice Boltzmann Model for Anisotropic Crystal Growth from Melt,” Journal of Statistical Physics 107, 1, 173-186 (2002).
[9] S. Chen, H.D. Chen, D. Martinez, and W. Matthaeus, “Lattice Boltzmann model for simulation of magnetohydrodynamics,” Phys. Rev. Lett. 67, 27, 3776-3779 (1991).
[10] S. Succi, M.Vergassola, and R. Benzi, “Lattice Boltzmann scheme for two-dimensional magnetohydrodynamics,” Phys. Rev. A 43, 4521 (1991).
[11] X.Y. Kang, D.H. Liu, J. Zhou, and Y.J. Jin, “Simulation of blood flow at vessel bifurcation by lattice Boltzmann method,” Chinese Physics Letters. 22, 11, 2873 (2005).

[12] M. Bernaschi, S. Melchionna, S. Succi, M. Fyta, E. Kaxiras, and J.K. Sircar, "A parallel Multi PHYsics/scale code for high performance bio-fluidic simulations," Computer Physics Communications. 180, 9, 1495-1502 (2009).
[13] Z.L. Guo, and T.S. Zhao, "Lattice Boltzmann model for incompressible flows through porous media," Physical Review E. 66 (32B), 036301-036304 (2002).
[14] S. Succi, E. Foti, and F. Higuera, "Three-dimensional flows in complex geometries with the lattice Boltzmann method," EPL (Europhsics Letters). 10, 5, 433 (2007).
[15] P. Prestininzi, A. Montessori, M. la. Rocca, and S. Succi, "Reassessing the single relaxation time Lattice Boltzmann Method for the simulation of Darcy´s flows," International Journal of Modern Physics C, 27, 04, 1650037 (2016).
[16] H.D. Chen, S. Kandasamy, S. Orszag, R. Shock, S Succi, and V. Yakhot "Extended Boltzmann kinetic equation for turbulent flows," Science. 301, 633-636 (2003).
[17] Z.H. Xia, Y.P. Shi, Y. Chen, M.R. Wang, and S.Y. Chen, "Comparisons of different implementations of turbulence modelling in lattice Boltzmann method," Journal of Turbulence. 16, 1, 67-80 (2015).
[18] H. Yu, L.S. Luo, and S.S. Girimaji, "Scalar mixing and chemical reaction simulations using lattice Boltzmann method," International Journal of Computational Engineering Science. 3, 1, 73-87 (2002).
[19] T. Inamuro, T. Ogata, and S. Tajima, "A lattice Boltzmann method for incompressible two phase flows with large density differences," Journal of Computational Physics. 198, 2, 628-644 (2004).
[20] A. Montessori, G. Falcucci, M. la Rocca, S. Ansumali, and S. Succi, "Three-Dimensional Lattice Pseudo-Potentials for Multiphase Flow simulations at High Density Ratios," Journal of Statistical Physics. 161, 6, 1404-1419 (2015).
[21] M. Sbragaglia, and S. Succi, "Analytical calculation of slip flow in lattice Boltzmann models with kinetic boundary conditions," Physics of Fluids. 17, 093602 (2005).
[22] A. Montessori, P. Prestininzi, M. la Rocca, and S. Succi, "Lattice Boltzmann approach for complex nonequilibrium flows," Physical Review E. 92, 043308 (2015).
[23] S. Gabbaneli, G. Drazer, and J. Koplik, "Lattice Boltzmann method for non-Newtonian fluids," Physical Review E. 72, 046312 (2005).
[24] M. La Rocca, A. Montessori, P. Prestininzi and S. Succi, "A multispeed Discrete Boltzmann Model for transcritical 2D shallow water flows," Journal of Computational Physics. 284, 117-132 (2015).
[25] Z.H. Chai and B.C. Shi, "A novel lattice Boltzmann model for the Poisson equation," Applied Mathematical Modelling. 32, 10, 2050-2058 (2008).
[26] Y.L. Duan, and R.X. Liu, "Lattice Boltzmann model for two-dimensional unsteady Burgers' equation," Journal of Computational and Applied Mathematics. 206, 1, 432-439 (2007).
[27] G.W. Yan, "A lattice Boltzmann equation for waves," Journal of Computational Physics. 161, 1, 61-69 (2000).
[28] J.Y Zhang, G.W. Yan, and Y.F. Dong, "A new lattice Boltzmann model for the Laplace equation," Applied Mathematics and Computation. 215, 2, 539-547 (2009).
[29] C.F. Ma, "A new lattice Boltzmann model for kdv-burgers equation," CHIN.PHYS.LETT. 22 (9), 2313 (2005).
[30] Y.L. Duan, L. R.X. Liu, and Y.Q. Jiang, "Lattice Boltzmann model for the modified Burgers' equation." Applied Mathetics and Computation. 202, 2, 489-497 (2008).
[31] G.W. Yan, Y.S. Chen, and S.X. Hu, "Simple lattice Boltzmann model for simulating flows with shock wave," Physical Review E. 59, 454 (1999).
[32] J.Y. Zhang, and G.W. Yan, "Lattice Boltzmann method for one and two-dimensional Burgers equation," Physica A. 387, 19-20, 4471-4786 (2008).
[33] F.J. Higuera, and J. Jimenez, "Boltzmann approach to lattice gas simulation," Europhysics letters. 9 (7), 663-668 (1989).

[34] F.J. Higuera, S. Succi, and R. Benzi, "Lattice gas dynamics with enhanced collisions," Europhysics Letters. 9, 7, 345-349 (1989).
[35] Y.H. Qian, D. d´Humières, and P. Lallemand, "Lattice BGK models for Navier-Stokes equation," Europhysics Letters. 17, 6, 479-484 (1992).
[36] Bhatnagar P L, Gross E P, Krook M., "A model for collision processes in gases. I. Small amplitude processes in charged and neutral one-component systems," Physical Review, 94, 511-525 (1954)
[37] D. d'Humières, "Multiple-relaxation-time lattice Boltzmann models in three dimensions," Philos Trans A Math Phys Eng Sci. 15, 360, 1792:437-51 (2002).
[38] Z. Li, M. Yang, and Y.W. Zhang, "Lattice Boltzmann method simulation 3D natural convection with double MRT model," International Journal of Heat and Mass Transfer, 94, 222-238 (2016).
[39] J. Latt, and B. Chopard, "Lattice Boltzmann method with regularized pre-collision distribution functions," Mathematics and Computers in Simulation, 72, 2-6 (2006).
[40] A. Montessori, G. Falcucci, P. Prestinizi, M. la Rocca, and S. Succi, "Regularized lattice Bhatnagar-Gross-Krook model for two and three-dimensional cavity flow simulations," Physical Review E. 89, 053317 (2014).
[41] S. Succi, "Lattice Boltzmann 2038," EPL (Europhysics Letters). 109, 50001 (2015).
[42] J.D. Sterling, and S.Y. Chen, "Stability Analysis of Lattice Boltzmann Methods," Journal of Computational Physics. 123, 196-206 (1996).
[43] M.K. Banda, W.A. Yong, and A. Klar, "A stability notion for lattice Boltzmann equations," SIAM J. Sci. Comput. 27, 6, 2098-2111 (2006).
[44] R.W. Mei, D.Z Yu, and S.Y. Wei, "An accurate curved boundary treatment in the lattice Boltzmann method," Journal of Computational Physics. 161, 680-699 (1999).
[45] Z.L. Guo, C.G. Zheng, and B.C. Shi, "Non-equilibrium extrapolation method for velocity and boundary conditions in the lattice Boltzmann method," Chinese Physics. 11, 4, 0366-0374 (2002).
[46] Y. Chen, Z.H. Xia and Q.D. Cai, "Lattice Boltzmann method with tree structured mesh and treatment of curved boundaries," Chinese Journal of Computational Physics. 27, 1, 23-30 (2010).
[47] R.W. Mei, L.S. Luo, and W. Shyy, "Force Evaluation in the Lattice Boltzmann Method Involving Curved Geometry," Phys. Rev. E 65, 041203, 2002.
[48] Z.L. Guo, C.G. Zheng, and B.C. Shi, "An extrapolation method for boundary conditions in lattice Boltzmann method," Physics of Fluids. 14, 6, 2007-2010 (2002).
[49] T. Vassilis, "On the resolution of critical flow regions in inviscid linear and nonlinear instability calculations," Journal of Engineering Mathematics. 34, 111-129 (1998).
[50] M.G. Macaraeg, and C.L. Streett, "Improvements in spectral collocation discretization through a multiple domain technique," Applied Numerical Mathematics. 2, 2, 95-108 (1986).
[51] Mohamed A. Ramadan and Talaat S. El-Danaf, "Numerical treatment for the modified Burgers equation," Math. Comput. Simulat. 70, 2, 90-98 (2005).